Article:
Xia, X, Stewart, DI orcid.org/0000-0001-5144-1234, Cheng, L et al. (4 more authors) (2020) Changes in groundwater bacterial community during cyclic groundwater-table variations. Hydrological Processes, 34 (25). pp. 4973-4984. ISSN 0885-6087

https://doi.org/10.1002/hyp.13917

Changes in groundwater bacterial community during cyclic groundwater-table variations

Running title: Water-table variations affect bacteria

Xuefeng Xia[1,3], Douglas Ian Stewart[2], Lirong Cheng[1,3], Kai Wang[1,3], Jing Li[4], Dan Zhang[5], Aizhong Ding[1,3,*]

[1] Engineering Research Center of Groundwater Pollution Control and Remediation of Ministry of Education, College of Water Sciences, Beijing Normal University, Beijing 100875, China

[2] School of Civil Engineering, University of Leeds, Leeds LS2 9JT, UK

[3] Beijing Key Laboratory of Urban Hydrological Cycle and Sponge City Technology, College of Water Sciences, Beijing Normal University, Beijing 100875, China

[4] Shandong Refresher Env. Eng. & Consulting, Jinan 250022, China

[5] Beijing Municipal Research Institute of Environmental Protection, Beijing Key Laboratory for risk modeling and remediation of contaminated sites, Beijing 100037, China

* Corresponding author: Aizhong Ding. Present address: 12#, Xueyuannan Road, Haidian District, 100875 Beijing, PR China.

E-mail address:

xiaxuefengbnu@163.com (Xuefeng Xia)

D.I.Stewart@leeds.ac.uk (Douglas Ian Stewart)

l.cheng@bnu.edu.cn (Lirong Cheng)

wangkaik@mail.bnu.edu.cn (Kai Wang)

liju8445@163.com (Jing Li)

zhangdan@cee.cn (Dan Zhang)

ading@bnu.edu.cn (Aizhong Ding)

Acknowledgments

This work was supported by the National Natural Science Foundation of China (No. 41672227) and National Key R & D Program of China (No. 2018YFC1800905).

Abstract

Column experiments containing an aquifer sand were subjected to static and oscillating water tables to investigate the impact of natural fluctuations and rainfall infiltration on the groundwater bacterial community just below the phreatic surface, and its association with the geochemistry. Once the columns were established, the continuously saturated zone was anoxic in all three columns. The rate of soil organic matter (SOM) mineralization was higher when the water table varied cyclically than when it was static due to the greater availability of NO_3^- and SO_4^{2-}. Natural fluctuations in the water table resulted in a similar NO_3^- concentration to that observed with a static water table but the cyclic wetting of the intermittently saturated zone resulted in a higher SO_4^{2-} concentration. Rainfall infiltration induced cyclic water-table variations resulted in a higher NO_3^- concentration than those in the other two columns, and a SO_4^{2-} concentration intermediate between those columns. As rainwater infiltration resulted in slow downward displacement of the groundwater, it is inferred that NO_3^- and SO_4^{2-} were being mobilized from the vadose zone. NO_3^- was mainly released by SOM mineralization (which was enhanced by the infiltration of oxygenated rainwater), but the larger amount of SO_4^{2-} release required a second mechanism (possibly desorption). Different groundwater bacterial communities evolved from initially similar populations due to the different groundwater histories.

Keywords: Water-table variations; rainfall infiltration; natural fluctuations; SOM mineralization; NO_3^-; SO_4^{2-}; bacterial communities; groundwater histories

1. Introduction

Groundwater represents 95% of global freshwater and is thus an essential resource for drinking water, agriculture and industry (Igor, 1993). The microbial community in an aquifer can have a profound impact on groundwater quality, as microorganisms break down organic matter, consume oxygen, change the oxidation state of inorganic compounds, recycle nutrients and break down pollutants (Kim & Gadd, 2008). Thus, it is important to understand how microbial community varies as a function of location, and how its metabolic activity varies as a function of time (Griebler, Malard, & Lefébure, 2014).

The groundwater table in an aquifer can fluctuate in short-term, seasonally and from year to year in response to variations in rainfall infiltration, groundwater flow, groundwater extraction and recharge, surface water levels and other natural causes (Rühle, von Netzer, Lueders, & Stumpp, 2015; Haack et al., 2004; Krause, Bronstert, & Zehe, 2007; Dobson, Schroth, & Zeyer, 2007). This produces a zone of intermittent saturation immediately above the continuously saturated zone where there are cyclical variations in the redox state and geochemistry (Yang et al., 2017; Stegen et al., 2016). Saturation, redox state and geochemistry are the principal factors that shape the microbial community present at a location (Shade, Jones, & Mcmahon, 2008; Medihala, Lawrence, Swerhone, & Korber, 2012; Zheng et al., 2019). Thus, temporal heterogeneity associated with groundwater-table fluctuations will impose a selective pressure that will favor microorganisms possessing metabolic plasticity and redox tolerance mechanisms (Rosenberg & Freedman, 1994).

There have been numerous studies of the effect of groundwater-table variations on bacterial processes in aquifers, but most have focused on the fate of natural and anthropomorphic contaminants in the intermittently saturated zone of an aquifer (e.g. Banks, Clennan, Dodds, & Rice, 1999; Van Driezum et al., 2018). Unsurprisingly, these show that electron donor and acceptor availability determine both microbial community composition and biogeochemical processes that the community mediates (e.g. Braun, Schröder, Knecht, & Szewzyk, 2016). However, it is interesting to note that indigenous microorganisms exhibit greater activity in a region of groundwater table variation than they would in equivalent zones above a static groundwater table (Banks et al., 1999), possibly because alternative movements of groundwater table transport nutrients and air to zone where air- and water-filled pores co-exist creating microhabitats with optimized conditions for microbial activity (Rainwater, Mayfield, Heintz, & Claborn, 1993; Banks et al., 1999). Moreover, different causes of a rising groundwater table may result in different responses of the indigenous microbial populations in an aquifer, due to difference in water chemistry and water-flow pathway (Zhou, Kellermann, & Griebler, 2012). Local rainfall infiltration involves downward percolation of water from the atmosphere through vadose zone, potentially eluting solutes and natural organics, and the upward displacement of pore air from capillary fringe against the water flow direction (Rainwater et al., 1993). Whereas regional recharge of an aquifer can result in upward permeation of groundwater from saturated zone, which will displace the pore air from capillary fringe upwards ahead of the wetting front. Such differences must lead to different redox conditions, affect the activity of indigenous

93 microorganisms, and impact on the evolution of the groundwater microbial community
94 (Pett-Ridge & Firestone, 2005).
95 Microbial communities often require time to respond to environmental change (Rezanezhad,
96 Couture, Kovac, O'Connell, & Van Cappellen, 2014), particularly as metabolic responses to new
97 environment can themselves cause geochemical changes creating new ecological niches over
98 time (Broman, Sjöstedt, Pinhassi, & Dopson, 2017; Graham et al., 2016). Therefore, variations in
99 microbial community with the level of groundwater table depend on the period over which
100 groundwater table is varying. With short-duration rainfall events, a single cycle may only cause a
101 small change in microbial population (Steenwerth, Jackson, Calderón, Scow, & Rolston, 2005),
102 whereas slow seasonal changes in groundwater table can result in significant differences in DNA
103 "fingerprint" of microbial populations (Zhou, Zhang, Dong, Lin, & Su, 2015). However, with
104 more rapid wet/dry cycling, the geochemistry can evolve during initial cycles before a relatively
105 steady state is reached (RoyChowdhury et al., 2018; Park, Yang, Tsang, Alessi, & Baek, 2018),
106 suggesting that laboratory studies involving a single wet-dry cycle must be interpreted with
107 caution.
108 This study investigated temporal changes in the groundwater bacterial community during
109 cyclic groundwater-table variations in laboratory columns. Two different patterns of
110 groundwater-table variation were simulated and compared with a static groundwater table. These
111 represented rainfall infiltration (RI), and natural fluctuations (NF) in groundwater table resulting
112 from variations in regional extraction and recharge. The bacterial communities were determined
113 over three successive groundwater-table cycles and correlated with geochemical parameters to

114 determine how the bacterial community varied, both within a cycle and between cycles, as a
115 function of geochemistry.
116
117 **2. Materials and methods**
118 *2.1. Experimental system and groundwater-table variation procedure*
119 The pilot-scale aquifer columns, consisting of cylindrical acrylic vessels with a length of
120 120 cm and an internal diameter of 24 cm (Fig. 1), were established in the Water Sciences
121 laboratory at Beijing Normal University where the ambient temperature was typically 28 ± 0.5
122 °C. Fine-grained natural river sand was collected from uncontaminated floodplain sediments near
123 Cihe (Shijiazhuang, China). Prior to use, the sand was washed with tap water, dried at 105 °C for
124 10 h, and sieved < 0.25 mm. Properties of the sand are reported in Table 1(a). Aquifer columns
125 were packed with the sand using a wet-packing procedure (see the supplementary material). The
126 water was completely drained after packing, when the packed height was 110 cm, the compacted
127 density was 1.60 g cm^{-3}, and the effective porosity was 0.35. O_2-depleted tap water (prepared by
128 N_2 sparging for about 60 min; see Table 1(b)) was then injected from the column bottom using a
129 peristaltic pump until the groundwater table reached a position 40 cm above the bottom. In the
130 column with a static (ST) groundwater table, no further changes in the groundwater table were
131 imposed. In the other columns, a cyclic variation in the groundwater table was imposed.
132 In both NF and RI experiments, a static groundwater table was maintained for 12 h, then the
133 cyclic pattern was commenced. Three full groundwater-table cycles were conducted. In the first
134 step the groundwater table was raised to 80 cm above the bottom of the columns over a period of

100 h. With the NF experiments O_2-depleted tap water was pumped into the bottom of the column at a rate of 1.09 ml min^{-1} (see the supplementary material), whereas in the RI experiments tap water (see Table 1(b)) was injected into the top of the column using a second peristaltic pump (at the same flow rate). Subsequent steps were the same in the NF and RI experiments; the groundwater table was held static for 40 h, and then was lowered to 40 cm above the base over a period of 100 h by pumping groundwater out of the bottom of the columns (flow-rate 1.03 ml min^{-1}). The groundwater table was held static for 40 h between cycles and for 12 h after the last cycle. The intended pattern of groundwater-table variation during the NF and RI experiments is shown in Fig. 2. A straight-forward cyclic pattern was used to allow comparison between the two regimes, and between the cycles of the same column. However, it had a similar periodicity to variations that occur in the agricultural region of Central Hebei (part of the North China Plain) in response to (spring) irrigation and periodic heavy summer rainfall (Hebei has a temperate continental monsoon climate). The rate at which the water table was increased (0.4 cm/h) was a compromise between that observed in the Central Hebei during irrigation (~0.04 cm/h) and that anticipated in response to more intense monsoon rainfall. This created three zones within the columns, a continuously saturated zone from 0-40 cm above the bottom of the columns, a zone of intermittent saturation from 40-80 cm, and a vadose zone from 80-110 cm.

2.2. Groundwater sampling

Triplicate groundwater samples (30 mL) were collected from the ST, NF and RI columns after 12, 112, 152, 252, 292, 392, 432, 532, 572, 672, 712, 812 and 824 h (Fig. 2) using sampling

ports (VICI, USA) 30 cm above the base of the columns (Fig. 1; near the top of continuously saturated zone). Each sample was separated into two subsamples, which were used for geochemical and bacterial analysis, respectively.

2.3. Analytical methods

2.3.1 Geochemical analysis

The triplicate subsamples of each groundwater sample were filtered (< 0.45 μm Millipore), and stored at 4 °C for further analyses. Each subsample was analyzed less than 24 h after being collected. Dissolved organic carbon (DOC) was measured using a Vario TOC system (Elementar, Germany). NO_3^- and SO_4^{2-} were analyzed by ion chromatography (Dionex, America). Dissolved oxygen (DO) was measured at a height of 30 cm above the base of each column (near the top of continuously saturated zone) by an OXY-10 trace SMA technique (PreSens, Germany) with a DP-Pst3 dipping probe (PreSens, Germany) (details can be found in the supplementary material).

2.3.2 Bacterial community analysis

The triplicate subsamples of each groundwater sample were pooled for bacterial analysis, and labelled as ST1-ST13, NF1-NF13 and RI1-RI13 to indicate the experiment and the sample number (Fig. 2). Total DNA was extracted from 6 ml of groundwater using a TIANamp Bacteria DNA Kit (TIANGEN, China) following to the manufacturer's instructions (see the supplementary material for details). The V3-V4 hypervariable region of 16S rRNA gene was amplified by PCR using the broad specificity primers 338F (5'-ACTCCTACGGGAGGCAGCAG-3') and 806R (5'-GGACTACHVGGGTWTCTAAT-3') (Zhu et al., 2018). PCR conditions are described in the supplementary material. To reduce PCR

177 errors, amplification for each sample was performed in triplicate and mixed together, then the
178 amplicons were extracted from 2% agarose gels and purified by using the AxyPrep DNA Gel
179 Extraction Kit (Axygen Biosciences, USA) following the manufacturer's instructions, and
180 quantified using QuantiFluor™-ST (Promega, USA). Subsequently, all purified amplicons were
181 pooled in equimolar concentrations and were paired-end sequenced (2 × 300) on an Illumina
182 MiSeq PE300 sequencer (Illumina, USA) according to standard protocols at Allwegene
183 Technology Co., Ltd (Beijing, China).
184 The extraction of high-quality sequences was firstly performed with the QIIME package
185 (version 1.2.1). Raw sequences were selected based on sequence length, quality, primer and tag,
186 and low-quality sequences were removed (see the supplementary material). The high-quality
187 sequences were assigned operational taxonomic units (OTUs) under the threshold of 97%
188 identity using USEARCH (Version 10). Chimeric sequences were identified and removed using
189 USEARCH (version 10). OTUs with only one sequence (singleton) were not included in
190 downstream analysis, other OTUs were assigned to taxonomic groups using the Ribosomal
191 Database Project (RDP) classifier (version 2.2) against the Silva128 16S rRNA database using a
192 confidence threshold of 70%.
193 *2.4. Data analysis*
194 Analysis of OTU alpha diversity, including rarefaction (Fig. S1), and calculation of
195 Shannon index, was performed using Mothur package (version 1.34.4). Heat map was generated
196 from the relative abundances of top 20 OTUs after column-normalization using pheatmap
197 package in R (version 3.6.1). Based on the detrended correspondence analysis (DCA) result

198 (gradient length < 3.0), redundancy analysis (RDA) was used to investigate multivariate
199 correlations between the microbial populations and geochemical properties of the columns using
200 Canoco (version 4.5). The 100 most abundant OTUs across all the samples were identified, and
201 their relative abundances in each sample were log (x + 1) transformed for the RDA.
202
203 **3. Results**
204 *3.1. Geochemistry*
205 The DO concentrations near the top of continuously saturated zone showed the same
206 responses in the three columns, decreasing from an initial value of 2.5 mg L^{-1} to essentially zero
207 over a period of about 252 h. This corresponded with the end of the first groundwater-table cycle
208 in the NF and RI columns (Fig. 3a).
209 The DOC concentrations responded differently in the three columns. In the ST column,
210 DOC increased from an initial value of 3.5 mg L^{-1} to 7.1 mg L^{-1} after 112 h, then decreased to
211 3.8 mg L^{-1} after about 292 h, and finally remained steady at that value until the end of
212 experiments (824 h). The DOC in the NF column showed a cyclical response, which established
213 after the first increase in the groundwater table. Initially it exhibited little change over the first
214 112 h, then it increased while the groundwater table was static and while it was being lowered to
215 6.4 mg L^{-1} at the end of the cycle. During the subsequent groundwater-table cycles, DOC
216 decreased during the period when the groundwater table was rising and increased again during
217 the period when the groundwater table was static or falling. The DOC in the RI column exhibited
218 a slightly different cyclical response. It initially increased from 3.5 mg L^{-1} to 7.2 mg L^{-1} during

the first time when the groundwater table was rising. Thereafter, it increased during the period when the groundwater table was falling but decreased during the period when the groundwater table was static or rising (Fig. 3b).

The initial NO_3^- concentrations were about 4.0 mg L^{-1} in the three columns. In the ST column, NO_3^- increased to a value of 7.5 mg L^{-1} after 152 h, before decreasing to 0.4 mg L^{-1} after 824 h. In the NF column, the overall trend was a decrease in the NO_3^- concentration with time from its initial value to 0.3 mg L^{-1} after 824 h. However, there was a cyclic pattern imposed on this overall trend, the NO_3^- concentration decreased during the period when the groundwater table was static or rising, and increased when the groundwater table was being lowered. In the RI column, the pattern in the NO_3^- concentration was less clear, with largely an increasing trend to 8.0 mg L^{-1} during the first two groundwater-table cycles, and a decrease to 2.1 mg L^{-1} followed by recovery to 9.2 mg L^{-1} during the final cycle (Fig. 3c).

The initial SO_4^{2-} concentrations were about 42.0 mg L^{-1} in the three columns. In the ST column, this increased to a value of 151.3 mg L^{-1} after 152 h, and then decreased smoothly to 11.6 mg L^{-1} after 824 h. In the NF column, the SO_4^{2-} concentration exhibited a cyclical response, which established after the first increase in the groundwater table, where the SO_4^{2-} concentration increased when the groundwater table was lowered and decreased at it was raised, with an average of about 70 mg L^{-1} during the third groundwater cycle. The SO_4^{2-} concentration in the RI column exhibited a similar cyclical response, but with an average of about 40 mg L^{-1} during the third groundwater cycle (Fig. 3d).

239 *3.2. Bacterial community composition*

240 The diversity of the groundwater bacterial communities exhibits broadly same trend in the
241 three columns (Fig. 4). The Shannon diversity index remained broadly constant for the first 250
242 h, then decreased slowly over the next 300 h to about 50% of its initial value, before recovering
243 over ~100 h to broadly the initial value for the last 150 h of the experiments.

244 The initial populations of all three columns (ST1, NF1, RI1) clustered as small group in the
245 redundancy plot (Fig. 6), suggesting that these populations were similar. The distribution of
246 readings by phylum also indicates that these populations were similar (Fig. 5a). The initial
247 populations of the three columns were all dominated by readings within phyla Parcubacteria
248 (30-49%), Proteobacteria (21-33%), and Bacteriodetes (2-15%). The three most abundant OTUs
249 in each column contained ~20% of the readings (Table S1). In the ST column these OTUs were
250 all classified as Parcubacteria (OTU3 and OTU11 were candidate class Jorgensenbacteria,
251 OTU35 was unclassified class), whereas in the NF column they were OTU66 (genus
252 Rhodobacter in the class α-proteobacteria), OTU87 (genus Fluviicola in the phylum
253 Bacteroidetes) and OTU23 (unclassified class in the phylum Parcubacteria), and in the RI
254 column they were OTU4 (candidate class Jorgensenbacteria), OTU93 (Family Cryomorphaceae
255 in the phylum Bacteroidetes), and OTU23 (Table S2). 33 OTUs were abundant in all three
256 columns, representing typically a third of each population (Table S1).

257 The populations of the three column experiments at subsequent time points plotted in
258 different areas of the redundancy plot, suggesting divergence in their populations. After time
259 point 5 (the start of the second groundwater cycle), the populations of each column experiment

formed a loose cluster in slightly different regions of the redundancy plot (populations from the ST column formed the tightest cluster; Fig. 6). The distribution of readings by phylum exhibited a less clear trend over the first six time points, with as much variation between time points in the same column, as between different columns at the same time, but all the populations were dominated by phyla Parcubacteria and Proteobacteria (typically > 70% of all readings were from these phyla) (Fig. 5a). Three OTUs were amongst the 20 most abundant OTUs in > 75% of groundwater samples up to time point 6 (Fig. 5b, they were amongst the 100 most abundant OTUs in every sample, Table S1), two (OTU3 and OTU4) were classified as Parcubacteria (candidate class Jorgensenbacteria) and one (OTU1) was classified as Proteobacteria (genus Variovorax belonged to the class β-Proteobacteria).

At time point 9 (572 h), when the Shannon diversity index reached its minimum, all three columns were dominated by readings classified as proteobacteria (see Fig. 5a). At this time, 2/3rd of the readings in all three columns were from OTU2 (genus Pseudomonas belonged to the class γ-proteobacteria; 24-59%) and OTU1 (genus Variovorax; 11-49 %) mentioned above for its (albeit more modest) abundance at earlier time points. It should be noted that such increases in relative abundance may, in part, reflect a drop in overall bacterial abundance.

After time point 9, there were fewer common species amongst the abundant OTUs in groundwater samples from the three columns (Table S1). At time point 13 (824 h), 26 OTUs typically represented a third of the readings in each column. Further, a small number of highly abundant OTUs represented a quarter of the readings in each column, and these highly abundant OTUs were different (Table S1). In the ST column these were OTU3 (candidate class

281 Jorgensenbacteria, phylum Parcubacteria; 10%), OTU10 (order Clostridiales, phylum Firmicutes;
282 6%), an OTU9 (unclassified bacterium; 3%), OTU28 (genus Opitutus, phylum Verrucomicrobia;
283 3%), and OTU36 (family Nitrospiraceae, phylum Nitrospirae; 3%). In the NF column these were
284 OTU114 (family Comamonadaceae, class β-proteobacteria; 5%), OTU12 (genus Caulobacter,
285 class α-proteobacteria; 4%), OTU153 (genus Buchnera, class γ-proteobacteria; 3%), OTU69
286 (genus Azospirillum, class α-proteobacteria; 3%), OTU91 (genus Opitutus, phylum
287 Verrucomicrobia; 3%), OTU26 (genus Methyloversatilis, class β-proteobacteria; 2%), OTU33
288 (genus Novosphingobium, class α-proteobacteria; 2%), OTU138 (order Clostridiales, phylum
289 Firmicutes; 2%) and OTU1 (genus Variovorax; 2%). In the RI column these were OTU14 and
290 OTU34 (genus Desulfovirga, class δ-proteobacteria; 14% and 3%, respectively) and OTU27
291 (family Rhodocyclacea, class β-proteobacteria; 9%).
292 The RDA plot provided correlations between the groundwater bacterial communities and
293 the geochemical parameters (DO, DOC, NO_3^-, SO_4^{2-}). At time points 1-3 the bacterial
294 communities in all three columns were positively correlated with DO, but negatively correlated
295 thereafter. After time point 4, bacterial communities in the ST column were negatively correlated
296 with DOC and NO_3^-, while bacterial communities in the NF column were positively correlated
297 with SO_4^{2-} and negatively correlated with NO_3^- and DOC, and bacterial communities in the RI
298 column were positively correlated with DOC and NO_3^- and negatively correlated with SO_4^{2-}.
299

4. Discussion

The initial geochemical response in the continuously saturated soil below the oscillating zone (or the equivalent zone of the ST column) was similar in the three columns. The DO concentrations decreased continuously from 2.50 mg/L (~30% oxygen saturation) after column preparation, to below detection over the first 250 h in the three columns, and did not increase again despite the potential for air entrapment to occur with NF and RI. This indicates that once the columns were established the consumption of oxygen within the natural fine-grained river sand exceeded the O_2 flux to the continuously saturated zone regulated by entrapment, advection and diffusion (Dutta et al., 2015). The initial decrease in DO is the result of aerobic microbial metabolism coupled to oxidation of soil organic matter (SOM). The result was that the biogeochemistry of the continuously saturated zone was essential anoxic or anaerobic in the three columns after a time period that corresponded to the end of the first groundwater-table cycle in the NF and RI columns.

In the ST column, DOC increased from ~3.4 mg/L to ~7 mg/L over the first 100 h and then decreased steadily towards a steady-state value of ~3.8 mg/L after about 250 h. Such a DOC variation is a footprint of microbial activity (Malik & Gleixner, 2013), as DOC is released by microbial processing of SOM, although the labile hydrophilic neutral DOC fraction is itself readily metabolized (Kiikkilä, Kitunen, & Smolander, 2005; Steinbeiss, Temperton, & Gleixner, 2008; Miltner, Bombach, Schmidt-Brücken, & Kästner, 2012). The tap water used in these experiments contained ~3.4 mg/L DOC, which is likely to be a recalcitrant, hydrophobic acid DOC fraction that is only degradable on long time scales (Polimene et al., 2018; Kiikkilä et al.,

2005), and thus 3.4 mg/L DOC should be regarded as a baseline for interpreting DOC variations. The difference between the final and initial DOC concentrations may represent an increase in the amount of recalcitrant DOC in the column after the labile fraction of initial DOC pulse has been metabolized, or that there is an equilibrium between continued slow mineralization of SOM and subsequent DOC metabolism. The NO_3^- and SO_4^{2-} concentrations initially increased, but both peaked (at 152 h) shortly after the peak in DOC, and then gradually decreased with time as the saturated zone became more reducing. The initial release of NO_3^- and SO_4^{2-} from the soil was associated with increased microbial activity as the DO was consumed, whereas their subsequent decrease was the result of their consumption by anaerobic microorganisms as anoxia developed. Although SO_4^{2-} reduction coupled to organic matter oxidation is an important process in anaerobic systems (Zhou et al., 2015), it's interesting to find that SO_4^{2-} decreased under the presence of NO_3^-, which is consistent with the work of Song et al. (2019), who showed that SO_4^{2-} and NO_3^- were synchronously depleted with DOC decreasing.

In the NF column, DOC concentration decreased when the groundwater table was raised, while it increased when the groundwater table was static at its highest level, when it was lowered, and when it was static at its lowest level. In these experiments water was added or removed from the bottom of the column, displacing the groundwater upwards or downwards as a body. Thus, during an increase in the groundwater table the water at the level of sampling port was replaced by water from the zone just below it, and the displaced water was returned to the vicinity of sampling point when the groundwater table was subsequently lowered (Fig. 2 illustrates how the body of groundwater in the vicinity of the sampling port changes over time). If DOC

342 concentration is taken as an indicator of the rate of SOM mineralization (Song et al., 2018), then
343 initially there is a decrease in that rate with depth (DOC concentration in the vicinity of sampling
344 port decreased when the groundwater was displaced upwards and increased when it moved
345 downwards). The translocation of groundwater into a different region of soil matrix also seems to
346 increase the rate of DOC mineralization during the subsequent static period. This is probably a
347 transient effect resulting from the disequilibria associated with the introduction of different
348 groundwater bacteria and dissolved chemical species to SOM, chemical species and bacteria
349 associated with the soil matrix. However, it was sufficient to maintain a DOC concentration in
350 the groundwater near the phreatic surface that was consistently higher than that in the ST column.
351 The NO_3^- concentration in the vicinity of sampling port also decreased when the groundwater
352 was displaced upwards and increased when it moved downwards, but this pattern diminished
353 with time. After the first groundwater-table cycle the NO_3^- concentration in the NF column
354 followed a similar trend to that in the ST column, suggesting that anoxia developed at a similar
355 rate to the ST column and that only a small amount of additional NO_3^- was carried from the
356 intermittently saturated zone into the continuously saturated zone. As a result, most of NO_3^- had
357 been consumed after 800 h at an average rate similar to that during the ST experiments. Like the
358 NO_3^- concentration, the SO_4^{2-} concentration in the vicinity of sampling port decreased when
359 groundwater was displaced upwards and increased when it moved downwards, suggesting that
360 SO_4^{2-} concentration similarly decreased with depth near the phreatic surface. However, unlike
361 NO_3^- concentration, the magnitude of the in-cycle variations in SO_4^{2-} concentration was little
362 changed after three cycles, suggesting the local depth trend in the SO_4^{2-} concentration persisted

363 throughout the experiments. Moreover, the transition from SO_4^{2-} release when the groundwater
364 table was static at the lowest level during the first cycle, to SO_4^{2-} consumption when the
365 groundwater table was static at the lowest level during the third cycle, meant the average SO_4^{2-}
366 concentration was decreasing slightly with the increasing number of cycles. As in the ST column,
367 the initial release SO_4^{2-} from the soil was associated with increased microbial activity as the DO
368 was consumed (it's detection at the sampling port was delayed by the position of the
369 groundwater table). This was probably due to desorption or dissolution of inorganic S from soil
370 minerals in the intermittently saturated zone, although mineralisation of organic S (either
371 C-bonded S or ester-bonded sulphates) might also be contributing (Edwards, 1998). The net
372 decrease in SO_4^{2-} concentration from the end of cycle 1 to the end of cycle 3, and particularly the
373 decrease when the groundwater table was static during cycle 3, were the result of sulphate
374 reduction by anaerobic microorganisms as anoxia developed.
375 The DOC response in the RI column was initially indistinguishable from the ST column,
376 but subsequently exhibited a clear cyclic pattern from the point where the groundwater table was
377 first lowered from its highest level. This pattern was an increase in DOC concentration during
378 the period when the groundwater table was being lowered, a rapid decrease when the
379 groundwater table was static at its lowest level, and a slower decrease when the groundwater
380 table was being increased or static at its highest level. Tap water was injected into the top of the
381 column, but groundwater was removed from the bottom of column. Thus, during an increase in
382 the groundwater table, the groundwater in the vicinity of sampling port remained static, but was
383 replaced by the simulated rainfall from the intermittently saturated zone when the groundwater

table was subsequently lowered (Fig. 2). Thus, the increase in DOC when the groundwater table was lowered is an indication that the rate of SOM mineralization in the intermittently saturated zone was higher than that in the continuously saturated zone in ~100 h after it had been inundated with the simulated rainfall. This is associated with the transport of electron acceptors, such as DO in the simulated rainfall and NO_3^- eluted from the vadose zone to the intermittently saturated zone. The rate of decrease in DOC concentration through the subsequent stages of the groundwater-table cycle (when groundwater in the vicinity of sampling port was static) reflects a steady decrease in the rate of SOM mineralization with time (rainfall infiltration into the intermittently saturated zone later in the cycle may have had a second order effect through diffusive transport of electron acceptors from the recently saturated zone). The cyclic variations in NO_3^- and SO_4^{2-} concentrations differed slightly between cycles, but the dominant pattern was an increase in concentration when the groundwater table was lowered, and predominantly of consumption when the groundwater table was static or increasing. Thus NO_3^- was consumed in the continuously saturated zone when the groundwater table was static and replenished when the simulated rainfall was drawn down into the continuously saturated zone. The mechanism of NO_3^- replenishment might involve eluting soluble NO_3^- from the vadose zone or the intermittently saturated zone (Huebsch et al., 2014), but almost certainly also involved mineralization of organic-N. Mineralisation of nitrogen is most rapid when soil is warm, moist and well aerated (Johnson, Albrecht, Kettrings, Beckman, & Stockin, 2005), so is likely to be enhanced by periodic inundation by DO containing rainfall. The SO_4^{2-} concentration decreased slightly with successive groundwater-table cycles. Like the other columns, the initial increase of SO_4^{2-}

concentration was associated with increased microbial activity as the DO was consumed. Similarly, the mechanism was probably desorption or dissolution of inorganic S from soil minerals, although mineralisation of organic S might also be contributing (Edwards, 1998). However, the variation in the SO_4^{2-} concentration with time differed from the ST column because each rainfall event mobilised further SO_4^{2-} from the vadose zone, but the downward movement of the groundwater with each cycle prevented SO_4^{2-} accumulating near phreatic surface as it did in the NF columns.

The RDA ordination indicates that the groundwater bacterial communities diverged with time from initially similar populations due to groundwater-table variations (waterborne bacteria are subset of the bacteria in the columns, but bacteria attached to the soil particles were not analysed). The initial populations were dominated by phyla Parcubacteria, Proteobacteria and Bacteriodetes, which are widely found in marine and terrestrial environments (Sun et al., 2019; León-Zayas et al., 2017). The gradual decrease in bacterial community diversity over the first two groundwater cycles (time points 1-9) was the result of the selective pressure of rapidly developing anoxia (Humbert & Dorigo, 2005) and the dominance of OTUs from the initial bacterial communities immediately being able to exploit the resulting ecological niche. At time point 9, the dominant populations of all three columns were from the genera Pseudomonas and Variovorax. Pseudomonas are facultative anaerobes capable of heterotrophic denitrification using a variety of carbon substrates (Wu et al., 2019; Dolan et al., 2020), and Variovorax genus includes species capable of denitrification and sulphate reduction (Crevecoeur, Vincent, Comte, & Lovejoy, 2015). The subsequent increase in diversity of each column and the further

426 divergence in their populations are then due to differences in relative competitiveness of the
427 species present as they adapt to the evolving geochemistry of each column by metabolic
428 regulation (Ayuso, Acebes, López-Archilla, Montes, & Guerrero, 2009). The final bacterial
429 population of the ST column was dominated by OTU3 (10% of all readings) and OTU10 (6% of
430 all readings). The first, which was also abundant in the initial population, was classified as a
431 Parcubacteria, a phylum of poorly characterised fermentative anaerobes (León-Zayas et al.,
432 2017). The second, which had low abundance in any of the columns until the start of the third
433 groundwater cycle, was classified as a Clostridiales, an order of fermentative obligate anaerobes
434 (Stackebrandt, 2014). Other highly abundant OTUs in the ST13 (together making up 25% of the
435 population) were closely related to anaerobic nitrate reducers (opitutus; Chin, Liesack, & Janssen,
436 2001) or sulphate reducers (currently known anaerobes within the Nitrospiraceae family are all
437 within the genus Thermodesulfovibrio; Daims, 2014).
438 The NF column had the most diversity amongst the highly abundant OTUs at time point 13,
439 with three different α-proteobacteria, three different β-proteobacteria, a clostridia, a
440 γ-proteobacteria and a Verrucomicrobia representing 25% of all readings. Based on their
441 similarity to well-characterised species, this population is likely to contain both facultative and
442 obligate anaerobes, including species capable of nitrate and sulphate reduction (Willems, 2014;
443 Chin et al., 2001; Smalley et al., 2015; Kaksonen, Spring, Schumann, Kroppenstedt, & Puhakka,
444 2007). What is really notable about these OTUs is that most were not abundant in the NF and RI
445 columns until the third groundwater cycle and not at all in the ST column (the exceptions were
446 OTU1, Variovorax, which was ubiquitous throughout all three column experiments, and OTU114,

447 Comamonadaceae family, which was briefly abundant in the ST5). This suggests that it can take
448 several groundwater cycles for the bacterial populations to evolve to fully exploit the
449 geochemical conditions produced by a varying water-table, possibly because the geochemistry
450 itself varies during the cycles.

451 The final bacterial population of the RI column had the least diversity amongst the highly
452 abundant OTUs, with just three OTUs representing 25% of the population. Two were classified
453 as Desulfovirga (a sulfate-reducing strict anaerobe; Kaksonen et al., 2007) within the class
454 δ-proteobacteria (OTU14 and OTU34; 14% and 3%, respectively), and the other was classified
455 to the family Rhodocyclaceae (OTU27; 9%) within the class β-proteobacteria (a disparate class
456 of mainly facultative anaerobic bacteria that includes many nitrate reducers; Oren, 2014). Other
457 abundant OTUs (OTU117 and OTU28, each representing ~2% of the population) were closely
458 related to anaerobic nitrate reducers (Thrash, Ahmadi, Torok, & Coates, 2010; Chin et al., 2001).

459 In summary, the RDA indicates that the bacterial populations of all three columns evolved
460 slightly differently over the course of the experiments, presumably as each community adapted
461 to its specific geochemical environment. However, the principal species in time point 13 suggest
462 that the population of the ST column has evolved the least (the most abundant OTU was
463 abundant in the initial population), and the high abundance of a probable fermentative species
464 (OTU10) may reflect the lower concentration of electron acceptors, such as sulphate and nitrate,
465 that support anaerobic respiration. The RDA indicates that populations of the NF and RI columns
466 differed from each other at time point 13, which may reflect the low nitrate, but elevated sulphate
467 concentrations in the NF column, and elevated nitrate, but moderate sulphate concentrations in

468 the RI column. However, nitrate and sulphate reducers appeared to be abundant in both bacterial
469 populations, perhaps indicating that even the modest nitrate release from the intermittently
470 saturated influenced the bacterial population of the NF column.
471
472 **5. Conclusions**
473 A cyclically varying groundwater table in an uncontaminated fine-grained natural river sand
474 representative of aquifer soils increased the rate of SOM mineralization in the continuously
475 saturated zone immediately below the intermittently saturated zone in comparison with a control
476 experiment with a static groundwater table. This was an anoxic zone, and enhanced
477 mineralization appeared to be associated with greater availability of electron accepting
478 compounds, particularly NO_3^- and SO_4^{2-}. When variations in the groundwater table resulted from
479 natural fluctuations, NO_3^- was consumed at similar rate to that observed with a static
480 groundwater table. SO_4^{2-} was also consumed but was replenished by periodic wetting of the
481 intermittently saturated zone. However, when the varying groundwater table resulted from
482 rainfall infiltration, NO_3^- was consumed when the groundwater table was static, but was
483 replenished when the simulated rainfall percolated down into the continuously saturated zone.
484 The mechanism of NO_3^- replenishment might involve eluting soluble NO_3^- from the vadose zone,
485 but almost certainly also involved mineralization of organic-N, which was likely to be enhanced
486 by periodic inundation by DO containing rainfall.
487 The RDA ordination indicated that the groundwater bacterial communities at the top of
488 continuously saturated zone of the NF and RI columns diverged from the ST column with time

from initially similar populations due to groundwater-table variations. However obvious differences in the most abundant OTUs in the three experiments only emerged after two complete groundwater cycles (~500 h). In conclusion, variations in the water table and, furthermore, the local flow direction during recharge have a strong influence on the geochemistry and microbiology of the groundwater bacterial community just below the phreatic surface of an aquifer.

Declarations of competing interest

None.

Data availability statement

The data used to support the findings of this study are available from the corresponding authors upon reasonable request.

Supporting file legend

Supplementary Material.

References

Ayuso, S. V., Acebes, P., López-Archilla, A. I., Montes, C., & Guerrero, M. C. (2009). Environmental factors controlling the spatiotemporal distribution of microbial communities in a coastal, sandy aquifer system (Doñana, southwest Spain). *Hydrogeology Journal*, *17*(4),

767-780.

Banks, M. K., Clennan, C., Dodds, W., & Rice, C. (1999). Variations in microbial activity due to fluctuations in soil water content at the water table interface. *Journal of Environmental Science & Health Part A*, *34*(3), 479-505.

Braun, B., Schröder, J., Knecht, H., & Szewzyk, U. (2016). Unraveling the microbial community of a cold groundwater catchment system. *Water Research*, *107*, 113-126.

Broman, E., Sjöstedt, J., Pinhassi, J., & Dopson, M. (2017). Shifts in coastal sediment oxygenation cause pronounced changes in microbial community composition and associated metabolism. *Microbiome*, *5*, 96.

Chin, K. J., Liesack, W., & Janssen, P. H. (2001). Opitutus terrae gen. nov., sp. nov., to accomodate novel strains of the division 'Verrucomicrobia' isolated from rice paddy soil. *International Journal of Systematic and Evolutionary Microbiology*, *51*, 1965-1968.

Crevecoeur, S., Vincent, W. F., Comte, J., & Lovejoy C. (2015). Bacterial community structure across environmental gradients in permafrost thaw ponds: methanotroph-rich ecosystems. *Frontiers in Microbiology*, *6*, 192.

Daims, H. (2014). The Family Nitrospiraceae. In: E. Rosenberg, E. F. DeLong, S. Lory, E. Stackebrandt, & F. Thompson (Eds.), *The Prokaryotes* (pp. 733-749). Heidelberg, Berlin: Springer.

Dobson, R., Schroth, M. H., & Zeyer, J. (2007). Effect of water-table fluctuation on dissolution and biodegradation of a multi-component, light nonaqueous-phase liquid. *Journal of Contaminant Hydrology*, *94*(3-4), 235-248.

Dolan, S. K., Kohlstedt, M., Trigg, S., Vallejo Ramirez, P., Kaminski, C. F., Wittmann, C., & Welch, M. (2020). Contextual flexibility in Pseudomonas aeruginosa central carbon metabolism during growth in single carbon sources. *mBio*,*11*(2), e02684-19.

Dutta, T., Carles-Brangarí, A., Fernàndez-Garcia, D., Rubol, S., Tirado-Conde, J., & Sanchez-Vila, X. (2015). Vadose zone oxygen (O_2) dynamics during drying and wetting cycles: An artificial recharge laboratory experiment. *Journal of Hydrology*, *527*, 151-159.

Edwards, P. J. (1998). Sulfur cycling, retention, and mobility in soils: A review. *USDA, General Technical Report NE-250*.

Graham, E., Crump, A. R., Resch, C. T., Fansler, S., Arntzen, E., Kennedy, D., … Stegen, J. C. (2016). Coupling spatiotemporal community assembly processes to changes in microbial metabolism. *Frontiers in Microbiology*, *7*, 1949.

Griebler, C., Malard, F., & Lefébure, T. (2014). Current developments in groundwater ecology-from biodiversity to ecosystem functioning and services. *Current Opinion in Biotechnology*, *27*, 159-167.

Haack, S. K., Fogarty, L. R., West, T. G, Alm, E. W., Mcguire, J. T., Long, D. T., … Forney, L. J. (2004). Spatial and temporal changes in microbial community structure associated with recharge-influenced chemical gradients in a contaminated aquifer. *Environmental Microbiology*, *6*(5), 438-48.

Huebsch, M., Fenton, O., Horan, B., Hennessy, D., Richards, K. G., Jordan, P., … Blum, P. (2014). Mobilisation or dilution? Nitrate response of karst springs to high rainfall events. *Hydrology and Earth System Sciences*, *11*(4), 4131-4161.

552 Humbert, J. F., & Dorigo, U. (2005). Biodiversity and aquatic ecosystem functioning: A mini
553 review. *Aquatic Ecosystem Health & Management*, *8*(4), 367-374.
554 Igor, S. (1993). World fresh water resources. In: P. H. Gleick (Ed.) *Water in crisis: A guide to the*
555 *world's fresh water resources*. Oxford, New York: Oxford University Press.
556 Johnson, C., Albrecht, G., Kettrings, Q., Beckman, J., & Stockin, K. (2005). Nitrogen basics-the
557 nitrogen cycle. *Agronomy Fact Sheet Series, Fact Sheet 2.* Cornell University, Cooperative
558 Extension.
559 Kaksonen, A. H., Spring, S., Schumann, P., Kroppenstedt, R. M., & Puhakka, J. A. (2007).
560 Desulfurispora thermophila gen. nov., sp. nov., a thermophilic, spore-forming
561 sulfate-reducer isolated from a sulfidogenic fluidized-bed reactor. *International Journal of*
562 *Systematic and Evolutionary Microbiology*, *57*(5), 1089-1094.
563 Kim, B. H., & Gadd, G. M. (2008). Bacterial Physiology and Metabolism. New York: Cambridge
564 University Press.
565 Kiikkilä, O., Kitunen, V., & Smolander, A. (2005). Degradability of dissolved soil organic carbon
566 and nitrogen in relation to tree species. *FEMS Microbiology Ecology*, *53*(1), 33-40.
567 Krause, S., Bronstert, A., & Zehe, E. (2007). Groundwater-surface water interactions in a North
568 German lowland floodplain-Implications for the river discharge dynamics and riparian
569 water balance. *Journal of Hydrology*, *347*(3-4), 404-417.
570 León-Zayas, R., Peoples, L., Biddle, J. F., Podell, S., Novotny, M., Cameron, J., … Bartlett, D. H.
571 (2017). The metabolic potential of the single cell genomes obtained from the Challenger
572 Deep, Mariana Trench within the candidate superphylum Parcubacteria (OD1).

573 *Environmental Microbiology*, *19*(7), 2769-2784.
574 Malik, A., & Gleixner, G. (2013). Importance of microbial soil organic matter processing in
575 dissolved organic carbon production. *FEMS Microbiology Ecology*, *86*(1), 139-148.
576 Medihala, P. G., Lawrence, J. R., Swerhone, G. D. W., & Korber, D. R. (2012). Effect of
577 pumping on the spatio-temporal distribution of microbial communities in a water well field.
578 *Water Research*, *46*(4), 1286-1300.
579 Miltner, A., Bombach, P., Schmidt-Brücken, B., & Kästner, M. (2012). SOM genesis: Microbial
580 biomass as a significant source. *Biogeochemistry*, *111*(1-3), 41-55.
581 Oren, A. (2014). The Family Rhodocyclaceae. In: E. Rosenberg, E. F. DeLong, S. Lory, E.
582 Stackebrandt, & F. Thompson (Eds.), *The Prokaryotes* (pp. 975-998). Heidelberg, Berlin:
583 Springer.
584 Park, S. M., Yang, J. S., Tsang, D. C. W., Alessi, D. S., & Baek, K. (2018). Enhanced irreversible
585 fixation of cesium by wetting and drying cycles in soil. *Environmental Geochemistry &*
586 *Health*, *41*(1), 149-157.
587 Pett-Ridge, J., & Firestone, M. K. (2005). Redox fluctuation structures microbial communities in
588 a wet tropical soil. *Applied and Environmental Microbiology*, *71*(11), 6998-7007.
589 Polimene, L., Rivkin, R. B., Luo, Y. W., Kwon, E. Y., Gehlen, M., Peña, M. A., … Jiao, N. Z.
590 (2018). Modelling marine DOC degradation time scales. *National Science Review*, *5*(4),
591 468-474.
592 Rainwater, K., Mayfield, M. P., Heintz, C., & Claborn, B. J. (1993). Enhanced in situ
593 biodegradation of diesel fuel by cyclic vertical water table movement: Preliminary studies.

Water Environment Research, *65*(6), 717-725.

Rezanezhad, F., Couture, R. M., Kovac, R., O'Connell, D., & Van Cappellen, P. (2014). Water table fluctuations and soil biogeochemistry: An experimental approach using an automated soil column system. *Journal of Hydrology*, *509*, 245-256.

Rosenberg, D. B., & Freedman, S. M. (1994). Temporal heterogeneity and ecological community structure. *International Journal of Environmental Studies*, *46*(2-3), 97-102.

RoyChowdhury, T., Bramer, L., Hoyt, D. W., Kim, Y. M., Metz, T. O., McCue, L. A., … Bailey, V. (2018). Temporal dynamics of CO_2 and CH_4 loss potentials in response to rapid hydrological shifts in tidal freshwater wetland soils. *Ecological Engineering*, *114*, 104-114.

Rühle, F. A., von Netzer, F., Lueders, T., & Stumpp, C. (2015). Response of transport parameters and sediment microbiota to water table fluctuations in laboratory columns. *Vadose Zone Journal*, *14*(5), 12.

Shade, A., Jones, S. E., & Mcmahon, K. (2008). The influence of habitat heterogeneity on freshwater bacterial community composition and dynamics. *Environmental Microbiology*, *10*(4), 1057-1067.

Smalley, N. E., Taipale, S., De Marco, P., Doronina, N. V., Kyrpides, N., Shapiro, N., … Kalyuzhnaya, M. G. (2015). Functional and genomic diversity of methylotrophic Rhodocyclaceae: Description of Methyloversatilis discipulorum sp. nov. *International Journal of Systematic & Evolutionary Microbiology*, *65*(7), 2227-2233.

Song, N., Xu, H., Yan, Z., Yang, T., Wang, C., & Jiang, H. L. (2019). Improved lignin degradation through distinct microbial community in subsurface sediments of one eutrophic

615 lake. *Renewable Energy*, *138*, 861-869.
616 Song, Y. Y., Song, C. C., Hou, A. X., Ren, J. S., Wang, X. W., Cui, Q., & Wang, M. Q. (2018).
617 Effects of temperature and root additions on soil carbon and nitrogen mineralization in a
618 predominantly permafrost peatland. *Catena*, *165*, 381-389.
619 Stackebrandt, E. (2014). The Family Clostridiaceae, Other Genera. In: E. Rosenberg, E. F.
620 DeLong, S. Lory, E. Stackebrandt, & F. Thompson (Eds.), *The Prokaryotes* (pp. 67-73).
621 Heidelberg, Berlin: Springer.
622 Steenwerth, K. L., Jackson, L. E., Calderón, F. J., Scow, K. M., & Rolston, D. E. (2005).
623 Response of microbial community composition and activity in agricultural and grassland
624 soils after a simulated rainfall. *Soil Biology & Biochemistry*, *37*(12), 2249-2262.
625 Steinbeiss, S., Temperton, V. M., & Gleixner, G. (2008). Mechanisms of short-term soil carbon
626 storage in experimental grasslands. *Soil Biology & Biochemistry*, *40*(10), 2634-2642.
627 Stegen, J. C., Fredrickson, J. K., Wilkins, M. J., Konopka, A. E., Nelson, W. C., Arntzen, E.
628 V., … Tfaily, M. (2016). Groundwater-surface water mixing shifts ecological assembly
629 processes and stimulates organic carbon turnover. *Nature Communications*, *7*, 11237.
630 Sun, Y., Li, X., Liu, J. J., Yao, Q., Jin, J., Liu, X. B., & Wang, G. H. (2019). Comparative
631 analysis of bacterial community compositions between sediment and water in different
632 types of wetlands of northeast china. *Journal of Soils and Sediments*, *19*, 3083-3097.
633 Thrash, J. C., Ahmadi, S., Torok, T., & Coates, J. D. (2010). Magnetospirillum bellicus sp. nov.,
634 a novel dissimilatory perchlorate-reducing alphaproteobacterium isolated from a
635 bioelectrical reactor. *Applied and Environmental Microbiology*,*76*(14), 4730-4737.

636 Van Driezum, I. H., Chik, A. H. S., Jakwerth, S., Lindner, G., Farnleitner, A. H., Sommer, R., …
637 Kirschner, A. K. T. (2018). Spatiotemporal analysis of bacterial biomass and activity to
638 understand surface and groundwater interactions in a highly dynamic riverbank filtration
639 system. *Science of the Total Environment*, *627*, 450-461.
640 Willems, A. (2014). The Family Comamonadaceae. In: E. Rosenberg, E. F. DeLong, S. Lory, E.
641 Stackebrandt, & F. Thompson (Eds.), *The Prokaryotes* (pp. 771-851). Heidelberg, Berlin:
642 Springer.
643 Wu, Z. S., Xu, F., Yang, C., Su, X. X., Guo, F. C., Xu, Q. Y., … Chen, Y. (2019). Highly efficient
644 nitrate removal in a heterotrophic denitrification system amended with redox-active biochar:
645 A molecular and electrochemical mechanism. *Bioresource Technology*, *275*, 297-306.
646 Yang, Y. S., Li, P. P., Zhang, X., Li, M. J., Lu, Y., Xu, B., & Yu, T. (2017). Lab-based
647 investigation of enhanced BTEX attenuation driven by groundwater table fluctuation.
648 *Chemosphere*, *169*, 678-684.
649 Zheng, T. L., Deng, Y. M., Wang, Y. X., Jiang, H. C., O'Loughlin, E. J., Flynn, T. M., … Ma, T.
650 (2019). Seasonal microbial variation accounts for arsenic dynamics in shallow alluvial
651 aquifer systems. *Journal of Hazardous Materials*, *367*, 109-119.
652 Zhou, A. X., Zhang, Y. L., Dong, T. Z., Lin, X. Y., & Su, X. S. (2015). Response of the microbial
653 community to seasonal groundwater level fluctuations in petroleum
654 hydrocarbon-contaminated groundwater. *Environmental Science and Pollution Research*,
655 *22*(13), 10094-10106.

Zhou, Y. X., Kellermann, C., & Griebler, C. (2012). Spatio-temporal patterns of microbial communities in a hydrologically dynamic pristine aquifer. *FEMS Microbiology Ecology*, *81*(1), 230-242.

Zhu, F. X., Zhu, C. Y., Doyle, E., Liu, H. L., Zhou, D. M., & Gao, J. (2018). Fate of di (2 ethylhexyl) phthalate in different soils and associated bacterial community changes. *Science of the Total Environment*, *637-638*, 460-469.

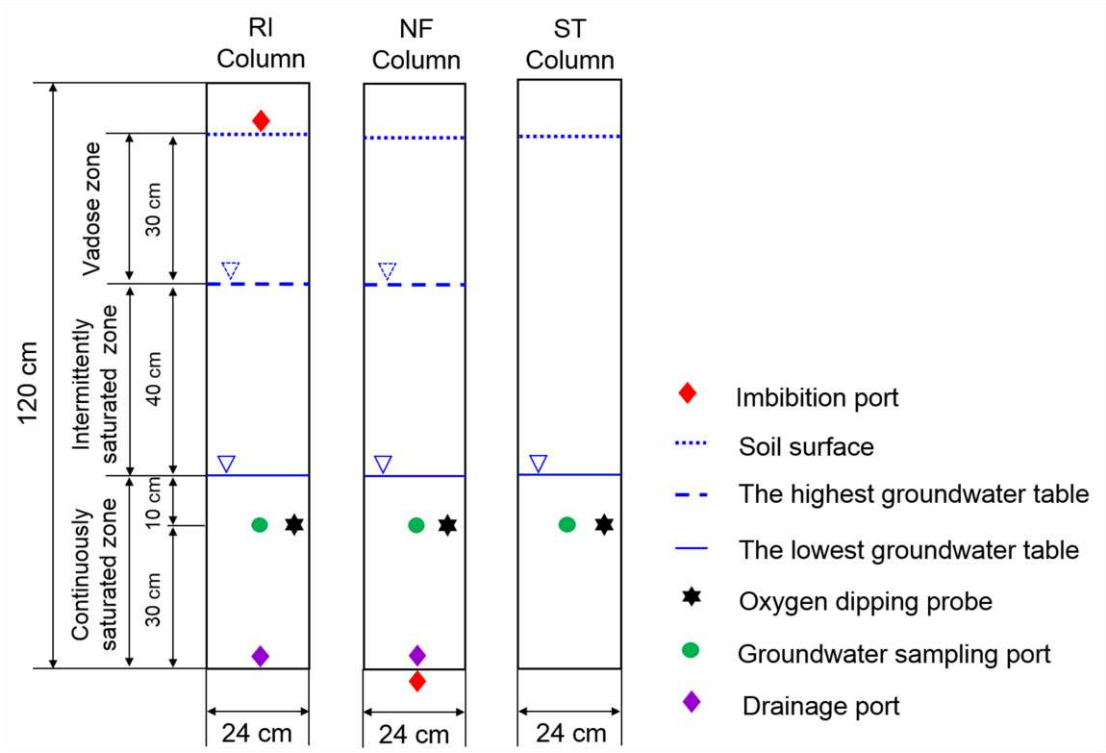

662

663 **Fig. 1.** Schematic of the experimental system showing the static (ST), natural fluctuations (NF),

664 and rainfall infiltration (RI) columns.

665

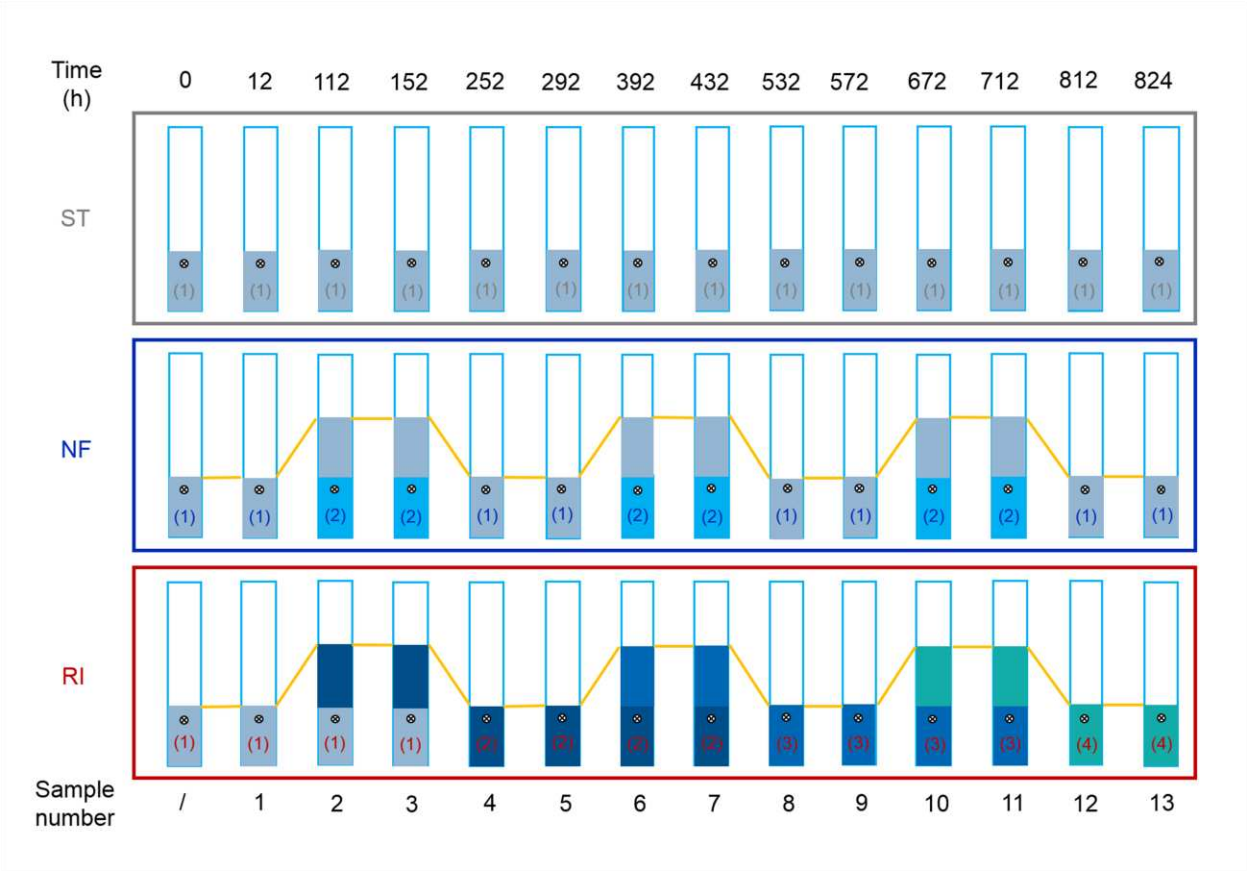

Fig. 2. Schematic representation of the experimental timelines showing the sampling points. The grey (1), light blue (2), mid-blue (3) and dark blue (4) shading represents the movement of the groundwater body in the static (ST), natural fluctuations (NF) and rainfall infiltration (RI) columns. Orange lines represent the intended pattern of groundwater-table in the NF and RI columns.

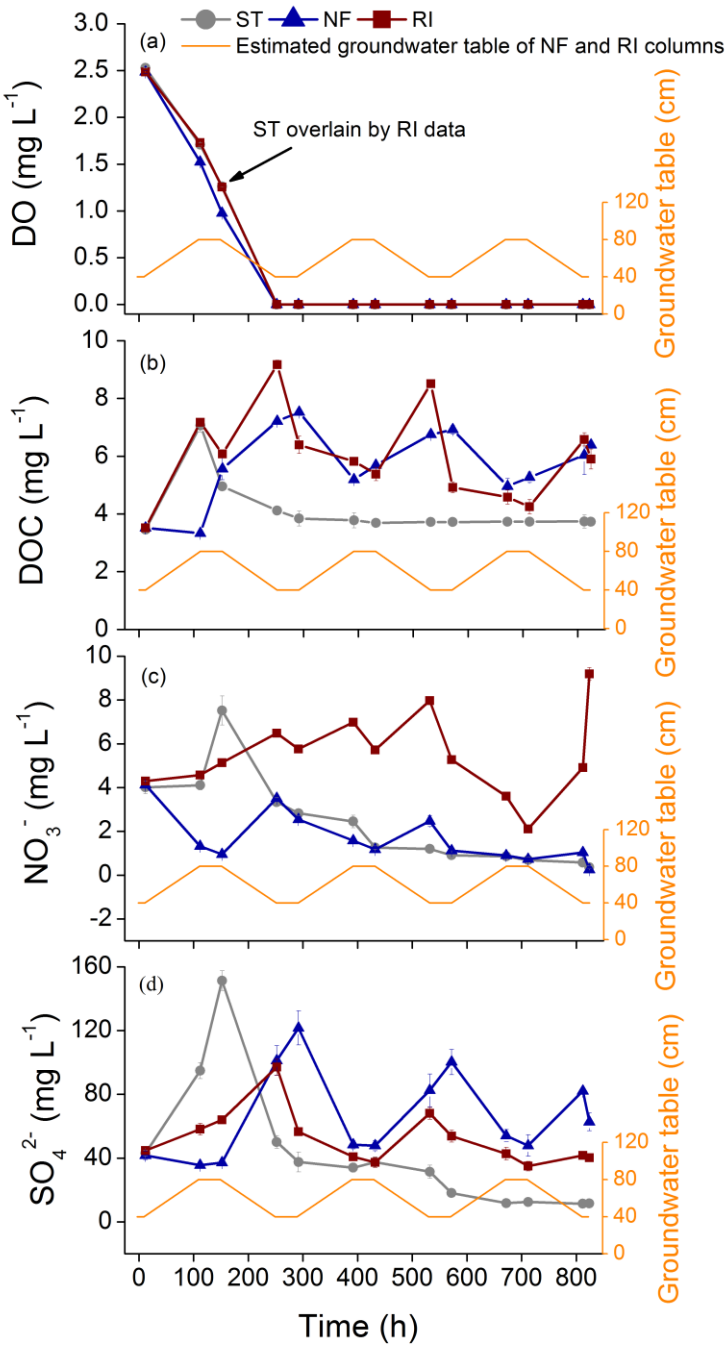

673

674 **Fig. 3.** Variations of (a) dissolved oxygen (DO); (b) DOC; (c) NO_3^- and (d) SO_4^{2-} in

675 groundwater samples from 10 cm below the surface of continuously saturated zone when the

676 water-table is static (ST), and when natural fluctuations (NF) and the rainfall infiltration (RI)

677 cause cyclic variations (the error bars represent the standard deviations of the mean values from

678 triplicate measurements).

679

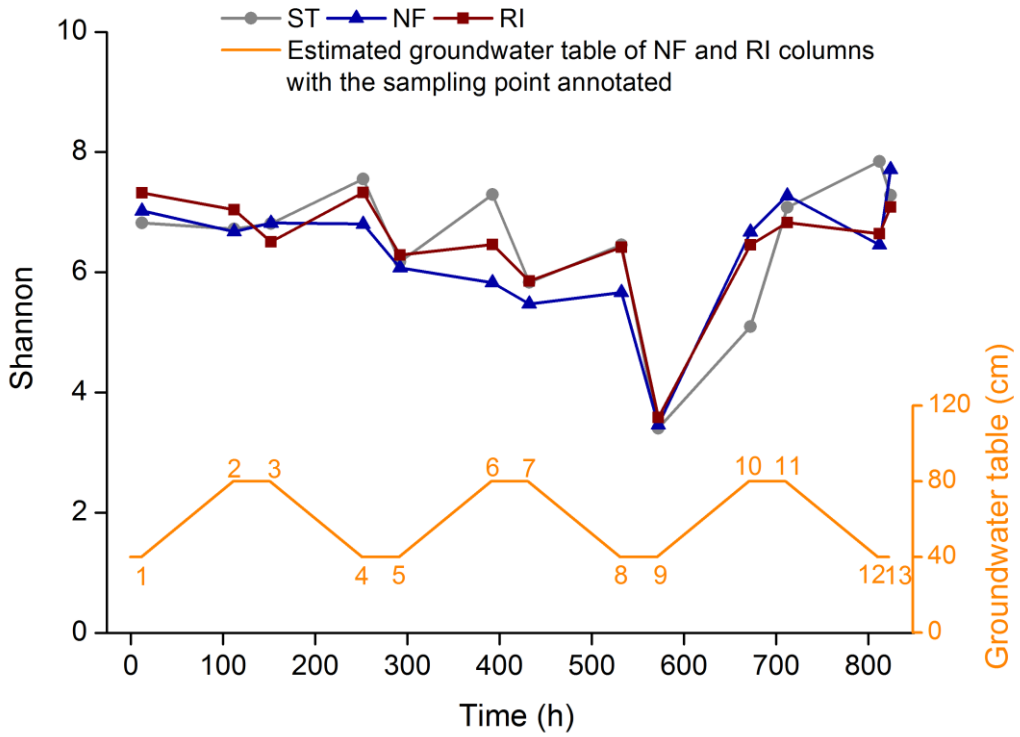

680

681 **Fig. 4.** Shannon index of bacterial community diversity in groundwater samples from 10 cm

682 below the surface of continuously saturated zone when the water-table is static (ST), and when

683 natural fluctuations (NF) and the rainfall infiltration (RI) cause cyclic variations.

684

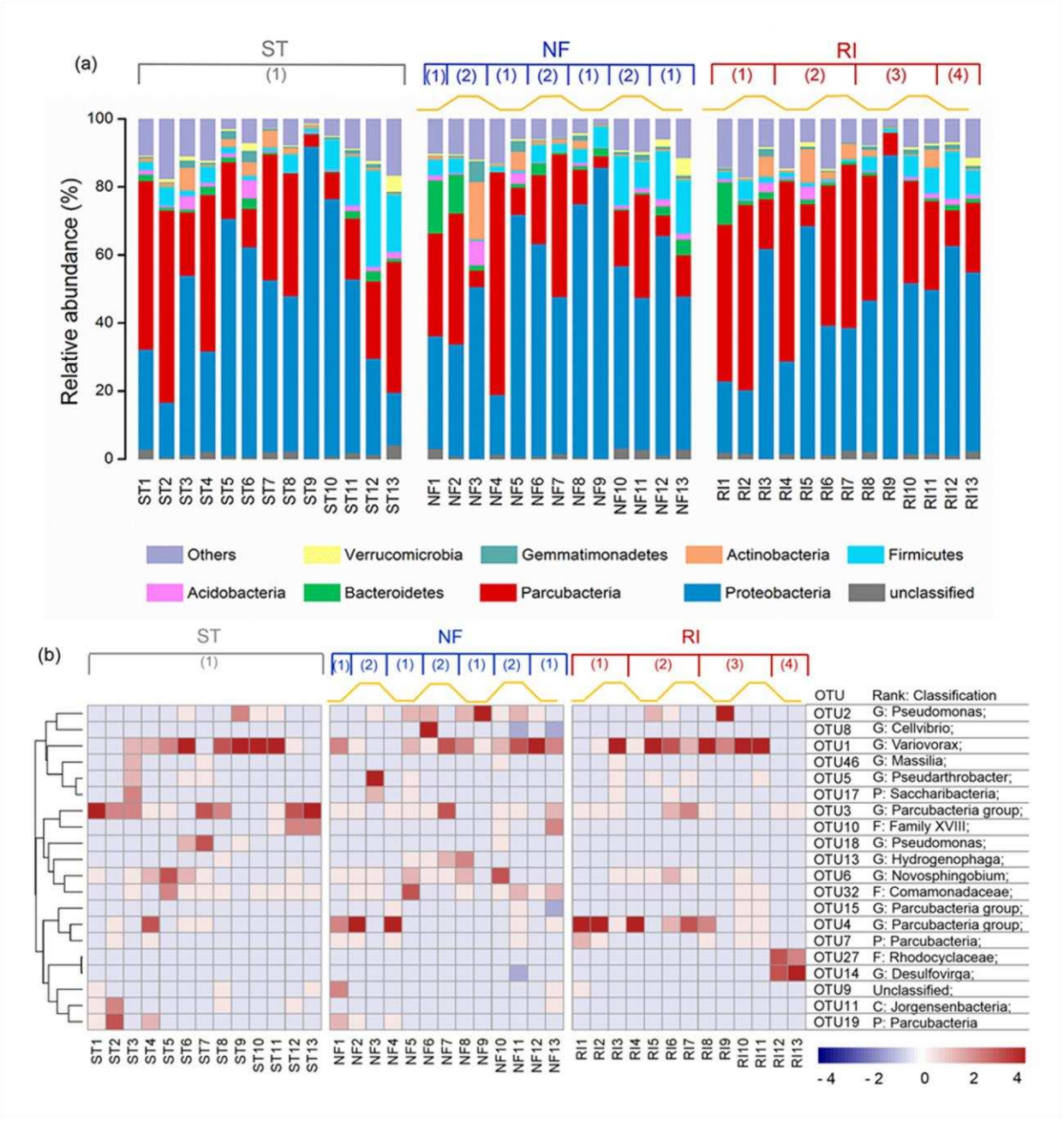

Fig. 5. (a) Relative abundance of the main phyla (relative abundance > 0.1 %) and (b) heat map of the 20 most abundant OTUs in groundwater samples from 10 cm below the surface of continuously saturated zone when the water-table is static (ST), and when natural fluctuations (NF) and the rainfall infiltration (RI) cause cyclic variations (heat map: red indicates high relative abundance and blue indicates low relative abundance). Orange lines at the top of (a) and (b) represent the intended pattern of groundwater-table in the NF and RI columns.

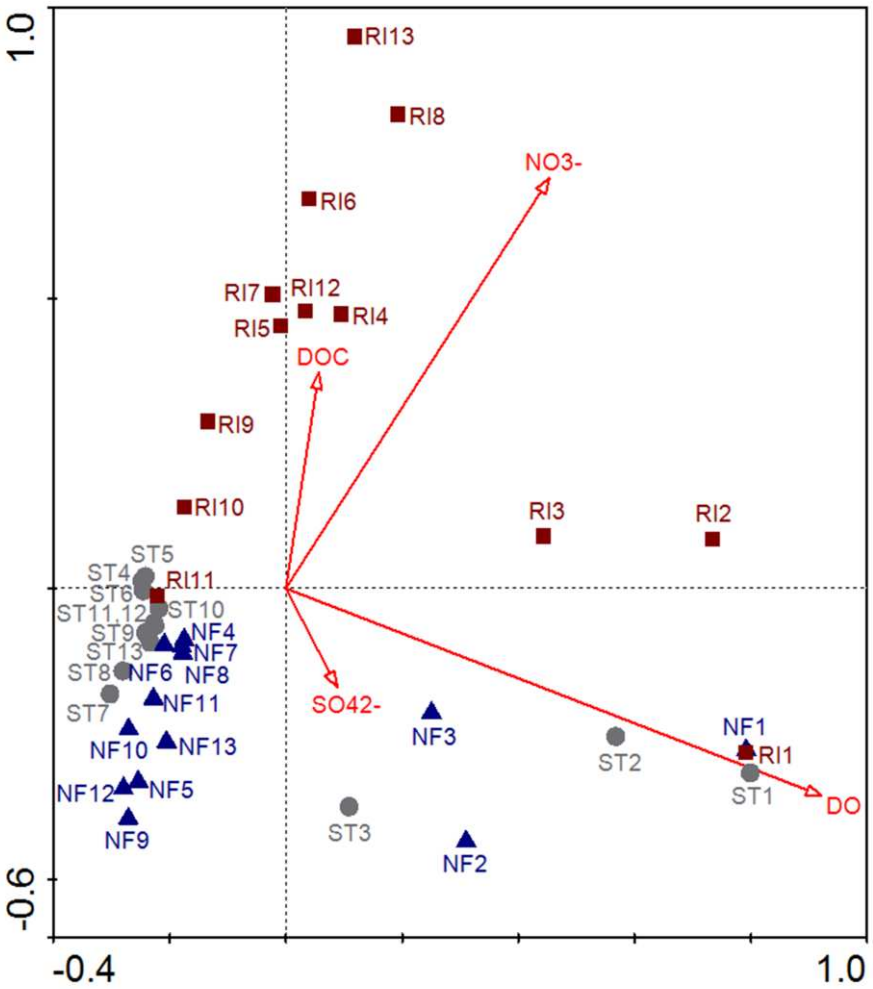

Fig. 6. Redundancy analysis (RDA) showing correlations between bacterial community structure and key geochemical parameters (bacterial community structure was represented by the relative abundance of the 100 most abundant OTUs across all samples). Grey circles, blue triangles and dark red squares represent the static (ST), natural fluctuations (NF) and rainfall infiltration (RI) columns, respectively.

699 Table 1:

700 (a) Basic properties of the fine-grained natural river sand.

Parameter		Value
Water saturation (%)		0.10
Bulk density (g cm^{-3})		1.32
TOC (g kg^{-1})		1.46
TN (g kg^{-1})		0.20
TS (g kg^{-1})		0.11
Size distribution (%)	< 0.02 mm	4.36
	0.02-0.1 mm	11.14
	0.1-0.25 mm	13.84
	0.25-1 mm	64.81
	> 1 mm	5.85

701 (b) Basic properties of the water.

Parameter		Value
DO (mg L^{-1})	oxygen-depleted tap water	1 ± 0.2
	tap water	8 ± 0.5
DOC (mg L^{-1})		3.39
NO_3^- (mg L^{-1})		3.71
SO_4^{2-} (mg L^{-1})		30.44

702